Bifurcations of Phase Portraits of a Singular Nonlinear Equation of the Second Class

A. S. Tchakoutio Nguetcho [a,c,*], Jibin Li [b,1], and J. M. Bilbault [c,2]

[a] *Laboratoire Interdisciplinaire des Sciences et Sciences Appliquées du Sahel (LISSAS), Département des Sciences Physiques, Université de Maroua, BP 46, Maroua-Cameroun*

[b] *Department of Mathematics, Zhejiang Normal University, Jinhua, Zhejiang, 321004, P. R. China and, Department of Mathematics, Kunming University of Science and Technology, Kunming, Yunnan, 650093 P. R. China*

[c] *Laboratoire LE2I UMR CNRS 6306, Aile des Sciences de l'ingénieur, Université de Bourgogne, BP 47870, 21078 Dijon Cedex, France*

Abstract

The soliton dynamics is studied using the Frenkel Kontorova (FK) model with non-convex interparticle interactions immersed in a parameterized on-site substrate potential. The case of a deformable substrate potential allows theoretical adaptation of the model to various physical situations. Non-convex interactions in lattice systems lead to a number of interesting phenomena that cannot be produced with linear coupling alone. In the continuum limit for such a model, the particles are governed by a Singular Nonlinear Equation of the Second Class. The dynamical behavior of traveling wave solutions is studied by using the theory of bifurcations of dynamical systems. Under different parametric situations, we give various sufficient conditions leading to the existence of propagating wave solutions or dislocation threshold, highlighting namely that the deformability of the substrate potential plays only a minor role.

Key words: Hamiltonian system, Nonlinear wave equation, non-convex interparticle interactions, deformability of the substrate potential, Solitary wave solution, Kink wave solution, Periodic wave solution, Breaking wave solution.

1 Introduction

Simplicity and universality are two key requirements of a good physical model. Universal models, which can be used to describe a variety of different phenomena, are very rare and yet are of major importance. They have been proved useful at several scales and moreover possess an educational value. A simple example of such models is the Frenkel Kontorova (FK) model [1]. The FK model has become very popular in many niches of solid state and nonlinear physics. They invented their model in order to describe the motion of a dislocation in crystals. Meanwhile, the FK model has also become a model for an adsorbate layer on the surface of crystal, for ionic conductors, for glassy materials, for charge-density-wave (CDW) transport, and for chains of coupled Josephson junctions. Especially, a number of current researches, such as sliding friction [2,3] , heat conduction [4–6] , chaos control and nonlinear coupled pendulum [7] are also carried out using the FK model.

The standard FK model describes a chain of coupled atoms subjected to an external periodic potential and its Hamiltonian is defined as

$$H = T + U. \tag{1}$$

T and U are the kinetic and potential energies respectively. U consists of interparticle interactions V_c that take into account the linear and nonlinear couplings between the nearest neighbors of the chain and the substrate external potential V_e along the chain with spatial period a. b stands for the natural spacing of the unperturbed chain. The contribution of the particle i to potential energy U is then defined as follows:

$$U\left(x_i\right) = V_c(r_i) + V_e\left(x_i\right), \quad 1 \leq i \leq n \tag{2}$$

where $r_i = x_{i+1} - x_i - b + a$ represents the distance between the nearest neighbors.

One of the basic restrictions of this traditional model adopted originally by the authors, which makes it applicable for small lattice misfits only, is the purely elastic interaction between neighboring atoms as a substitute for the real inter-atomic forces. In addition, in real physical systems, the shape of the

* Corresponding author.
Email addresses: nguetchoserge@yahoo.fr (A. S. Tchakoutio Nguetcho), lijb@zjnu.cn, jibinli@gmail.com (Jibin Li), bilbault@u-bourgogne.fr (J. M. Bilbault).
[1] This author is supported by the National Natural Science Foundation of China (10831003).
[2] This author is supported by the Regional Council of Burgundy.

substrate potential can deviate from the standard (sinusoidal or rigid) one and this may affect strongly the transport properties of the system.

As a better approach for modeling real systems, many researchers have considered the FK model while either modifying the external periodic potential [1] or modifying interactions between atoms [8–12]. For realistic anharmonic interactions, such as those of Toda, Morse, Markov and Trayanov, besides the position of the minimum there exists a second characteristic length at which the tensile strength of the bond reaches its maximum, that is the inflection point r_{inf}. This makes the behavior of such systems more complex. The mathematical challenges of solving the problem analytically increase since the equations are no more single valued. It has been reported in a numerical study of the discrete FK model with anharmonic interactions (Toda, Morse) [13] that beyond some critical values of the independent parameters (the natural lattice mismatch and/or amplitude of the external periodic potential), these equations have no solution which was interpreted as a disintegration of the system .

This work aims to consider a non-convex pair potential V_c [13–15] defined as :

$$V_c(r) = \frac{V_0 B\left(\frac{r}{r_0}\right)^2}{1 + B\left(\frac{r}{r_0}\right)^2} \tag{3}$$

with $r_0 = \frac{a}{2\pi}$. B changes the width of the potential well with depth V_0. It is a single non-convex even potential with a single minimum and infinitely differentiable. The curvature (elastic constant) of $V_c(r)$ is $2BV_0$ at $r = 0$, and $V_c(r)$ has inflection points at $\pm r_{inf} = \frac{r_0}{\sqrt{3B}}$. This potential, plotted

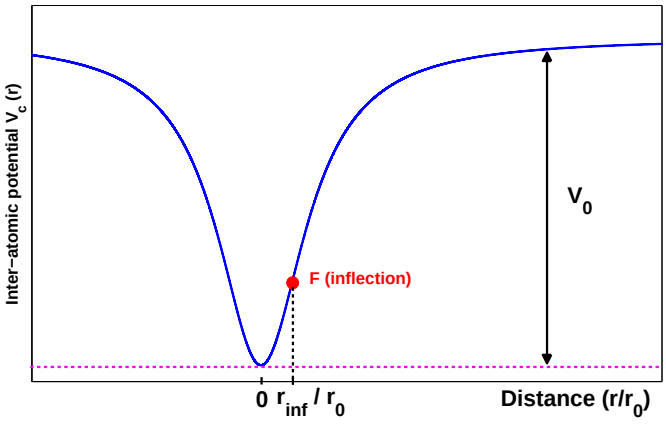

Fig. 1. Plot of the coupling potential $V_c(r)$

versus the nearest neighbors distance $\frac{r}{r_0}$ in Fig.1, is infinitely differentiable

and supposed to bear all qualitatively important features of the problem under the influence of a nonlinear periodic deformable substrate V_e.

For this purpose, we used an important type of on-site potential that describes many realistic situations (e.g., the dynamics of atoms adsorbed on crystal surfaces, Josephson jonctions, charge density wave condensate, $\cdots$) [1], that is:

$$V_e\left(x_i\right) = \varepsilon_s \frac{\sin^2\left(\dfrac{\pi x_i}{a}\right)}{\sigma^2 + \left(1-\sigma^2\right)\sin^2\left(\dfrac{\pi x_i}{a}\right)}, \tag{4}$$

where σ is related to the coefficient s introduced by Peyrard and Remoissenet [1] by $\sigma = \dfrac{1+s}{1-s}$. The parameter ε_s is the parameter that controls or adjusts the strength of the energy barriers of the substrate potential. In adsystem, ε_s is the activation energy for diffusion of an isolated adatom. At $\sigma = 1$ the potential $V_e(x_i, \sigma)$ has a sinusoidal shape, while at $\sigma < 1$, broad wells separate narrow barriers, and at $\sigma > 1$, deep narrow wells separate broad gently sloping barriers (see Fig. 2).

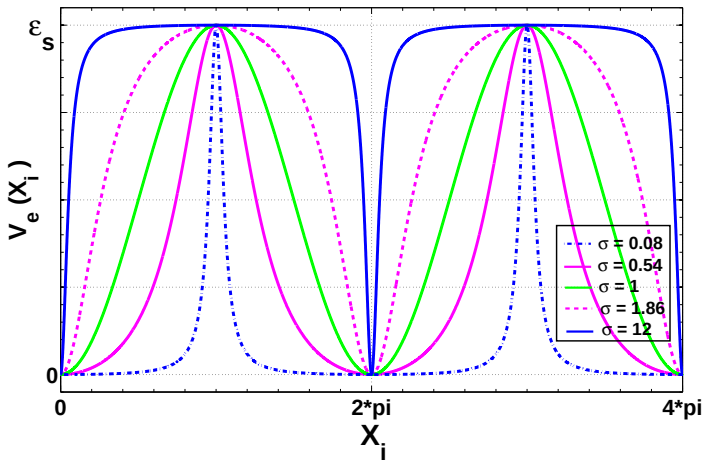

Fig. 2. Substrate potential $V_e(x_i)$ at different values of parameter σ

The next section will be devoted to the presentation of the equations and integrals of motion. The phase portraits will be presented in section 3, while the main behaviors of the wave solutions will be studied in (§4), followed by a summary and some conclusion remarks.

2 The equations of motion

The Hamiltonian for such a system is defined as:

$$H = A\sum_{i}^{n}\left\{\frac{1}{2}\left(\frac{d\phi_i}{dt}\right)^2 + \frac{C_0^2}{2b^2}\frac{\left(\phi_{i+1}-\phi_i-P\right)^2}{1+B\left(\phi_{i+1}-\phi_i-P\right)^2} + \right. \\ \left. + \omega_0^2\frac{\sin^2\left(\frac{\phi_i}{2}\right)}{\sigma^2+\left(1-\sigma^2\right)\sin^2\left(\frac{\phi_i}{2}\right)}\right\}, \qquad (5)$$

where $\phi_i = \frac{2\pi x_i}{a}$ is the scalar dimensionless displacement of particles, $P = 2\pi\left(\frac{b}{a}-1\right)$ stands for the natural lattice incompatibility between substrate and overlayer, while the factor $A = m\left(\frac{a}{2\pi}\right)^2$ sets the energy scale. The parameters C_0 and ω_0 are the characteristic velocity and frequency respectively, and are related to the non-convex dimensionless constant B (the parameter that controls the strength of the nonlinear coupling) and the amplitude of the substrate potential ε_s through $C_0^2 = \frac{2BV_0b^2}{A}$ and $\omega_0^2 = \left(\frac{2\pi}{a}\right)^2\frac{\varepsilon_s}{m}$. Finally, m represents the mass of atoms.

In the continuum limit, with dimensionless variables $X = \frac{x}{b}$ and $T = \omega_0 t$, when $\phi_i(t)$ is replaced by $\phi(X,T)$, the particles are governed by the following Euler-Lagrange equation:

$$\frac{\partial^2\phi}{\partial T^2} - \frac{C_0^2}{b^2\omega_0^2}\left[\frac{1-3B\left(\frac{\partial\phi}{\partial X}-P\right)^2}{\left[1+B\left(\frac{\partial\phi}{\partial X}-P\right)^2\right]^3}\right]\frac{\partial^2\phi}{\partial X^2} + \frac{1}{2}\frac{\sigma^2\sin(\phi)}{\left[\left(\sigma^2-1\right)\sin^2\left(\frac{\phi}{2}\right)-\sigma^2\right]^2} = 0. \qquad (6)$$

In extreme cases $B \to 0$ and $\sigma \to 1$, equation (6) leads to the well-known Sine Gordon equation. Using the independent propagating variable $u = X - vT$, where v is a constant velocity, (6) yields:

$$\left(\frac{1-3B\left(\frac{d\phi}{du}-P\right)^2}{\left[1+B\left(\frac{d\phi}{du}-P\right)^2\right]^3} - \mathbb{V}^2\right)\frac{d^2\phi}{du^2} = \frac{1}{2}\frac{\lambda\sigma^2\sin(\phi)}{\left[\left(\sigma^2-1\right)\sin^2\left(\frac{\phi}{2}\right)-\sigma^2\right]^2}, \qquad (7)$$

where $\mathbb{V} = \dfrac{vb\omega_0}{C_0}$ is a more suitable dimensionless expression to determine the velocity of the travelling waves. $d_0 = \dfrac{C_0}{\omega_0}$ is the characteristic length of the system, while $\lambda = \left(\dfrac{b}{d_0}\right)^2$ denotes the scaled amplitude of the periodic potential and measures the effective depth of the substrate potential of the system. The study of Eq. (7) can be best driven in the phase plane $\left(\phi, y = \dfrac{d\phi}{du}\right)$. Eq(7) can then be rewritten as:

$$\frac{d\phi}{du} = y, \quad \frac{dy}{du} = \frac{1}{2f\left(y\right)} \frac{\lambda\sigma^2 \sin\left(\phi\right)}{\left[\left(\sigma^2 - 1\right)\sin^2\left(\frac{\phi}{2}\right) - \sigma^2\right]^2}, \tag{8}$$

with

$$f(y) = \frac{1 - 3B(y-P)^2}{\left[1 + B(y-P)^2\right]^3} - \mathbb{V}^2. \tag{9}$$

If the function $f(y)$ has at least a real zero at $y = y_0$, (8) is a singular nonlinear system of the second class (see [17–19]). By using the transformation $du = f(y)d\xi$ when $y \neq y_0$, system (8) becomes the associated regular system as follows:

$$\frac{d\phi}{d\xi} = yf(y), \quad \frac{dy}{d\xi} = \frac{1}{2} \frac{\lambda\sigma^2 \sin\left(\phi\right)}{\left[\left(\sigma^2 - 1\right)\sin^2\left(\frac{\phi}{2}\right) - \sigma^2\right]^2} \equiv Q(\phi). \tag{10}$$

Systems (8) and (10) have the same first integral defined as:

$$\begin{aligned} H\left(\phi, y\right) &= \frac{\left(1 - 3BP^2\right)y^2 + 4BPy^3 - By^4}{\left(1 + BP^2\right)\left(1 + B(y-P)^2\right)^2} - \mathbb{V}^2 y^2 - \frac{2\lambda \sin^2\left(\frac{\phi}{2}\right)}{\left[\sigma^2 + \left(1 - \sigma^2\right)\sin^2\left(\frac{\phi}{2}\right)\right]} \\ &= h, \end{aligned} \tag{11}$$

where h is a constant.

System (10) is 2π-periodic in ϕ. Hence, the state (ϕ, y) can be viewed, for the main properties, on a phase cylinder $S^1 \times R$, where $S^1 =]-\pi, \pi]$ and $-\pi$ is identified with π (see Fig. 3).

Without loosing generality, we will assume in the following that σ is fixed, which leads to consider the systems (8) and (10) as four-parameter systems depending on $(B, \mathbb{V}, P, \lambda)$. The role of σ will be discussed later.

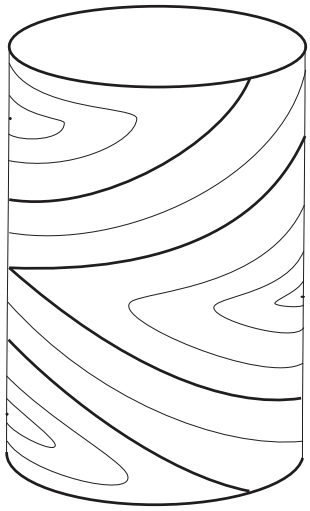

Fig. 3. The phase cylinder $S^1 \times R$ of system (10).

Obviously, $y = G(\phi)$ can not be derived explicitly from (11). Therefore, it is not possible to obtain explicit solutions by solving equation (7). However with the qualitative theory of differential equations, Eq. (7) can be solved and all related informations to its solutions can be derived, as well as phase portraits [20,21].

Let $Y = (y - P)^2$. For $\mathbb{V} \neq 0$, to find the zeros of function $f(y)$ is equivalent to find the roots of the cubic polynomial

$$\begin{aligned} F(Y) &= Y^3 + \frac{3}{B}Y^2 + \frac{3}{B^2}\left(1 + \frac{1}{\mathbb{V}^2}\right)Y + \frac{1}{B^3}\left(1 - \frac{1}{\mathbb{V}^2}\right) \\ &\equiv Y^3 + a_2 Y^2 + a_1 Y + a_0. \end{aligned} \tag{12}$$

Let $q = \frac{1}{3}a_1 - \frac{1}{9}a_2^2,\ r = \frac{1}{6}(a_1 a_2 - 3a_0) - \frac{1}{27}a_2^3$. Then, the discriminant $S = q^3 + r^2$ of cubic equation $F(Y) = 0$ is $S = \frac{1 + 4\mathbb{V}^2}{\mathbb{V}^6 B^6} > 0$. It follows that $F(Y)$ has only one real root $Y = Y_0$.

If and only if $a_0 < 0$, i.e., $0 < \mathbb{V} < 1$, the only real root Y_0 of cubic polynomial $F(Y)$ is positive. Then $f(y)$ has two real roots y_1 and y_2.

Therefore, for any $P \neq 0$, looking for the equilibrium points of system (10), we have the following conclusions:

(1) **For the static** $(\mathbb{V} = 0)$ **or subsonic velocity** $(0 < \mathbb{V} < 1)$ **cases:**
For $\mathbb{V} = 0$, $f(y)$ becomes zero for $y_1 = P + r_{inf}$, and $y_2 = P - r_{inf}$, while if $0 < \mathbb{V} < 1$, $y_1 = P - \sqrt{Y_0}$ and $y_2 = P + \sqrt{Y_0}$.
Then, for $(0 \leq \mathbb{V} < 1)$, there exist six equilibrium points of system (10) in the phase cylinder, at $O(0,0)$, $A(\pi,0)$, $B_1(0,y_1)$, $B_2(\pi,y_1)$, $C_1(0,y_2)$

and $C_2(\pi, y_2)$. On the straight lines $y = y_1$ and $y = y_2$, $\dfrac{dy}{du}$, defined by system (8), becomes infinite. These two straight lines are then two singular straight lines for system (8).

(2) **For the case of sonic velocities** $(\mathbb{V} = 1)$.
There exist four equilibrium points of system (10) at $O(0,0)$, $A(\pi,0)$, $B_1(0,P)$ and $B_2(\pi,P)$. On the straight lines $y = P$, $\dfrac{dy}{du}$, defined by system (8), becomes infinite. Thus, the straight line $y = P$ is a singular straight line for system (8).

(3) **For the case of supersonic velocities** $(1 < \mathbb{V} < \infty)$.
There exist two equilibrium points of system (10) at $O(0,0)$ and $A(\pi,0)$. In this case, because $f(y)$ has no real zero, system (8) is a regular dynamical system.

We notice that $f(0) = -\dfrac{\mathbb{V}^2 F(P^2) B^3}{(1+BP^2)^3}$.

(a) When $1 < \mathbb{V} < \infty$, $F(P^2) > 0$ and $f(0) < 0$.

(b) When $0 < \mathbb{V} < 1$, if $P^2 < Y_0$, then $f(0) > 0$, while if $P^2 > Y_0$, then $f(0) < 0$.

Let $M(\phi_i, y_j)$ be the matrix of the linearized approximation of system (10) at the equilibrium point (ϕ_i, y_j). Then, we have

$$\det M(\phi_i, y_j) = -Q'(\phi_i)[y_j f'(y_j) + f(y_j)],$$

where

$$f'(y) = \frac{12B\,(y-P)\left[B(y-P)^2 - 1\right]}{\left[B(y-P)^2 + 1\right]^4},$$

and $Trace\ M\,(\phi_i, y_j) = 0$.

Thus,

$$J(0,0) = \det M(0,0) = -\frac{\lambda}{2\sigma^2} f(0),$$

$$J(\pi,0) = \det M(\pi,0) = \frac{\lambda\sigma^2}{2} f(0),$$

$$J(0,y_j) = \det M(0,y_j) = -\frac{\lambda}{2\sigma^2} y_j f'(y_j),$$

$$J(\pi,y_j) = \det M(\pi,y_j) = \frac{\lambda\sigma^2}{2} y_j f'(y_j), \quad j = 1,2.$$

The theory of planar dynamical systems gives the following results for an equilibrium point of a planar integrable system:

- if $J < 0$, then the equilibrium point is a saddle point;
- If $J > 0$ then it is a center point;
- if $J = 0$ and the Poincaré index of the equilibrium point is 0, then this equilibrium point is a cusp [19,20].

For the Hamiltonian values defined by (11), we have

$$h_0 = H(0,0) = 0,$$

$$h_1 = H(\pi,0) = -2\lambda,$$

$$h_{2,3} = H(0,y_{1,2}) = \frac{(1-3BP^2)y_{1,2}^2 + 4BPy_{1,2}^3 - By_{1,2}^4}{(1+BP^2)\left(1+B(y_{1,2}-P)^2\right)^2} - \mathbb{V}^2 y_{1,2}^2,$$

$$h_{4,5} = H(\pi,y_{1,2}) = \frac{(1-3BP^2)y_{1,2}^2 + 4BPy_{1,2}^3 - By_{1,2}^4}{(1+BP^2)\left(1+B(y_{1,2}-P)^2\right)^2} - \mathbb{V}^2 y_{1,2}^2 - 2\lambda.$$

3 The phase portraits of the model

Note first that the case P and $-P$ are symmetric with respect to the ϕ-axe, which allows us to restrict our study to $P \geq 0$.

In order to solve the four-parameter systems (8) or (10), and to draw the portrait phases, we will discuss according the different cases $\mathbb{V} = 0$, $0 < \mathbb{V} < 1$, $\mathbb{V} = 1$ and $V > 1$. Using the above informations to perform qualitative analysis, we also represent in phase portraits the corresponding singular straight lines. They intersect transversally some families of orbits.

We should emphasize that when these singular straight lines of system (8)

exist, the vector fields defined by system (8) and system (10) are different. If an orbit of system (8) intersect a singular straight line $y = y_j$, that is $f(y_j) = 0$ in a particular point (ϕ_0, y_j), where ϕ_0 is not a multiple of π, then at this point, the second derivative $\dfrac{d^2\phi}{du^2}$ of $\phi(u)$ becomes infinite as shown by equation (7). The direction of vector field defined by system (8) changes rapidly to the inverse direction of the vector field defined by system (10). This lets the wave solution $\phi(u)$ of (7) associated with system (8) degenerate into a breaking solution, meaning physically a dislocation of the particle lattice, as we will show now.

Considering first the static case $\mathbb{V} = 0$, the coupling potential V_c can be rewritten as

$$\sum_i V_c\left(r_i\right) = \sum_i \frac{V_0 B\left(\phi_{i+1} - \phi_i - P\right)^2}{1 + B(\phi_{i+1} - \phi_i - P)^2}. \tag{13}$$

Deriving V_c versus ϕ_i gives the resulting force from the lattice on particle number i, namely

$$F_i = -2V_0 B\left[\frac{\phi_{i+1} - \phi_i - P}{\left[1 + B(\phi_{i+1} - \phi_i - P)^2\right]^2} - \frac{\phi_i - \phi_{i-1} - P}{\left[1 + B[\phi_i - \phi_{i-1} - P)^2\right]^2}\right] \tag{14}$$

Using the continuous media approximation $\left(\phi_{i+1} - \phi_i \to \dfrac{\partial\phi}{\partial X}\right)$ gives

$$F_i = -2V_0 B\frac{\partial^2\phi}{\partial X^2}\left[\frac{1 - 3B\left(\dfrac{\partial\phi}{\partial X} - P\right)^2}{\left[1 + B\left(\dfrac{\partial\phi}{\partial X} - P\right)^2\right]^3}\right] \tag{15}$$

This result shows that when $\dfrac{\partial\phi}{\partial X} = P \pm \dfrac{1}{\sqrt{3B}}$, the resulting force on particle i from the lattice vanishes. The attraction on particle i from the left neighbors is exactly balanced by the one from the right neighbors, resulting on a breaking of the lattice cohesion.

Note that the particle remains submitted to the substrate potential $V_e(x_i)$ (see Eq. (4)) but the links to their neighbors are broken.

Finally, with $y = \dfrac{\partial\phi}{\partial X} = \dfrac{d\phi}{du}$, (we recall that $u = X - vT = X$ for $\mathbb{V} = 0$), the lattice submits a dislocation when $f(y) = 0$, that is on the singular straight lines.

When $\mathbb{V} \neq 0$, the coupling potential must be replaced by an effective one,

taking into consideration the propagative variable $u = X - vT$. Then, dislocations occur when the slope $y = \dfrac{d\phi}{du}$ reaches one of the roots of $f(y) = 0$, when they exist. In the phase portraits, this corresponds to any intersection of the orbits with the singular straight lines, except at the minima of the potential $V_e(\phi_i)$.

(i) **Phase portraits in the static case ($\mathbb{V} = 0$) with $P = 0$**

For a given B, we have $y_1 = -y_2 = -\dfrac{1}{\sqrt{3B}}$, $h_2 = h_3 = \dfrac{1}{8B}$, $h_4 = h_5 = \dfrac{1}{8B} - 2\lambda$. Hence, when $\lambda = \dfrac{1}{16B}$, it follows that $h_4 = h_5 = h_0 = 0$. When λ increases, the cases $h_1 < 0 < h_4 < h_2$, $h_1 < h_4 = 0 < h_2$ and $h_1 < h_4 < 0 < h_2$ are successively obtained, as shown in Fig.4.

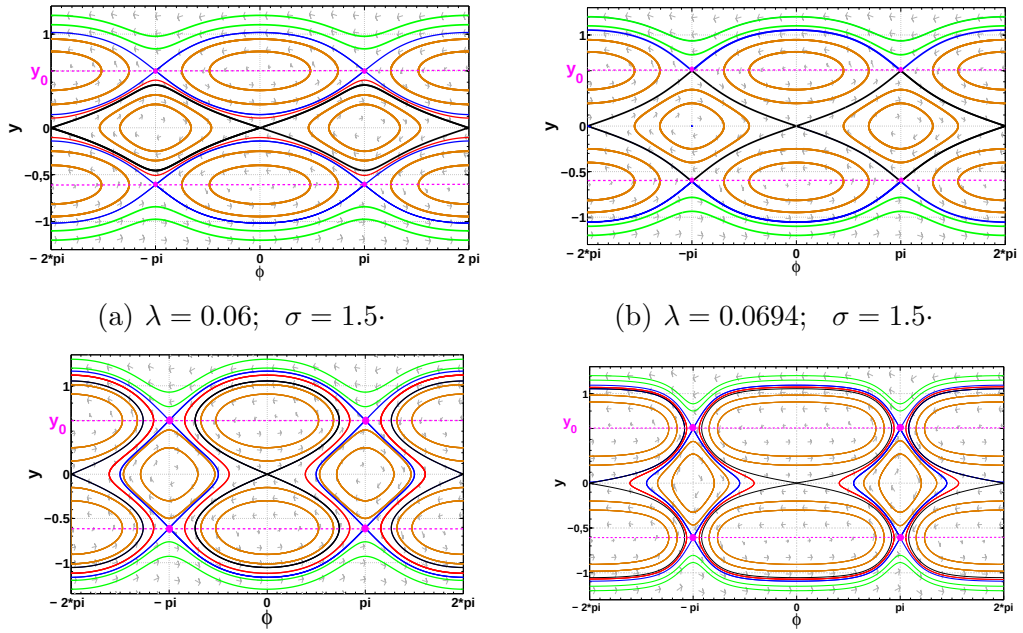

(a) $\lambda = 0.06$; $\sigma = 1.5$· (b) $\lambda = 0.0694$; $\sigma = 1.5$·

(c) $\lambda = 0.008$; $\sigma = 1.5$· (d) $\lambda = 0.008$; $\sigma = 3$·

Fig. 4. The bifurcation of phase portraits of system (10) for $\mathbb{V} = 0$, $P = 0$, $B = 0.9$, (a) $\lambda < \dfrac{1}{16B}$, (b) $\lambda = \dfrac{1}{16B}$, (c) $\lambda > \dfrac{1}{16B}$ and (d) $\lambda > \dfrac{1}{16B}$ but σ is now 3.

(ii) **Phase portraits of the subsonic velocity case** $(0 < \mathbb{V} < 1)$

In this case, there exist a fixed positive root Y_0 of $F(Y)$.

If $P = 0$, $y_{1,2} = \pm\sqrt{Y_0}$ and $h_2 = h_3 = \dfrac{Y_0(1 - BY_0)}{4(1 + BY_0)^2} - \mathbb{V}^2 Y_0, h_4 = h_5 = \dfrac{Y_0(1 - BY_0)}{4(1 + BY_0)^2} - \mathbb{V}^2 Y_0 - 2\lambda$. Let $\lambda_b = \dfrac{1}{2}\left(\dfrac{Y_0(1 - BY_0)}{4(1 + BY_0)^2} - \mathbb{V}^2 Y_0\right)$. It is easy to see that respectively the case $\lambda < \lambda_b$ ($\lambda = \lambda_b$, then $\lambda > \lambda_b$) leads to $h_1 < 0 < h_4 < h_2$ (respectively $h_1 < h_4 = 0 < h_2$, then

$h_1 < h_4 < 0 < h_2$), while these different phase portraits are shown in Fig.5.

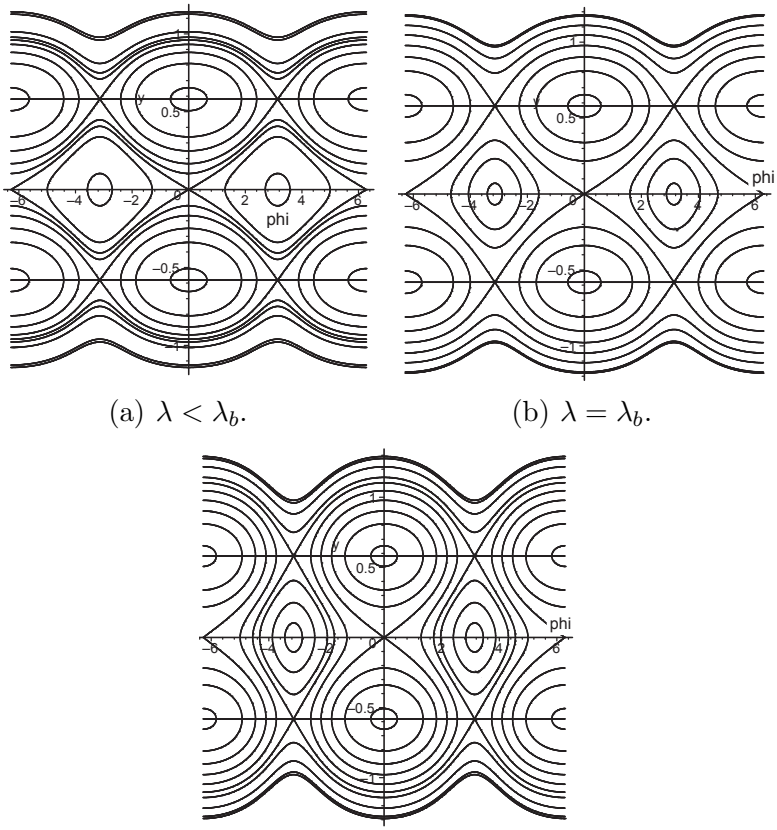

(a) $\lambda < \lambda_b$. (b) $\lambda = \lambda_b$.

(c) $\lambda > \lambda_b$.

Fig. 5. The bifurcation of phase portraits of system (10) for $P = 0$, $0 < \mathbb{V} < 1$. (Parameters: $B = 0.9$, $\mathbb{V} = 0.2$, $\sigma = 1.5$, (a) $\lambda = 0.025$, (b) $\lambda = \lambda_b = 0.03118632263$, (c) $\lambda = 0.05$.

If $P = \sqrt{Y_0}$, then $y_1 = 0$, $y_2 = 2Y_0$, $F(P^2) = 0$. Consequently $f(0) = 0$ and the two equilibrium points $O(0, 0)$ and $A(\pi, 0)$ are cusps.

When P varies from 0 to ∞, there exists a value $P = P_b$ such that $h_2 = h_5$. On Fig. 6, we present the phase portraits highlighting the bifurcations obtained when the parameter P increases.

(iii) **Phase portraits in the sonic velocity case** ($\mathbb{V} = 1$)

We have now $Y_0 = 0$, and $y_1 = y_2 = P$. The two equilibrium points $B_1(0, P)$ and $B_2(\pi, P)$ are cusps, and $h_{2,3} = -\dfrac{BP^4}{1 + BP^2}$. Thus, for a given parameter pair (B, λ), $h_1 = h_{2,3}$ when $P = P_a \equiv \lambda + \sqrt{\lambda^2 + \dfrac{2\lambda}{B}}$; we see in Fig. 7 the phase portraits for $P < P_a$, $P = P_a$ and $P > P_a$.

(iv) **Phase portraits in the supersonic velocity case** ($V > 1$)

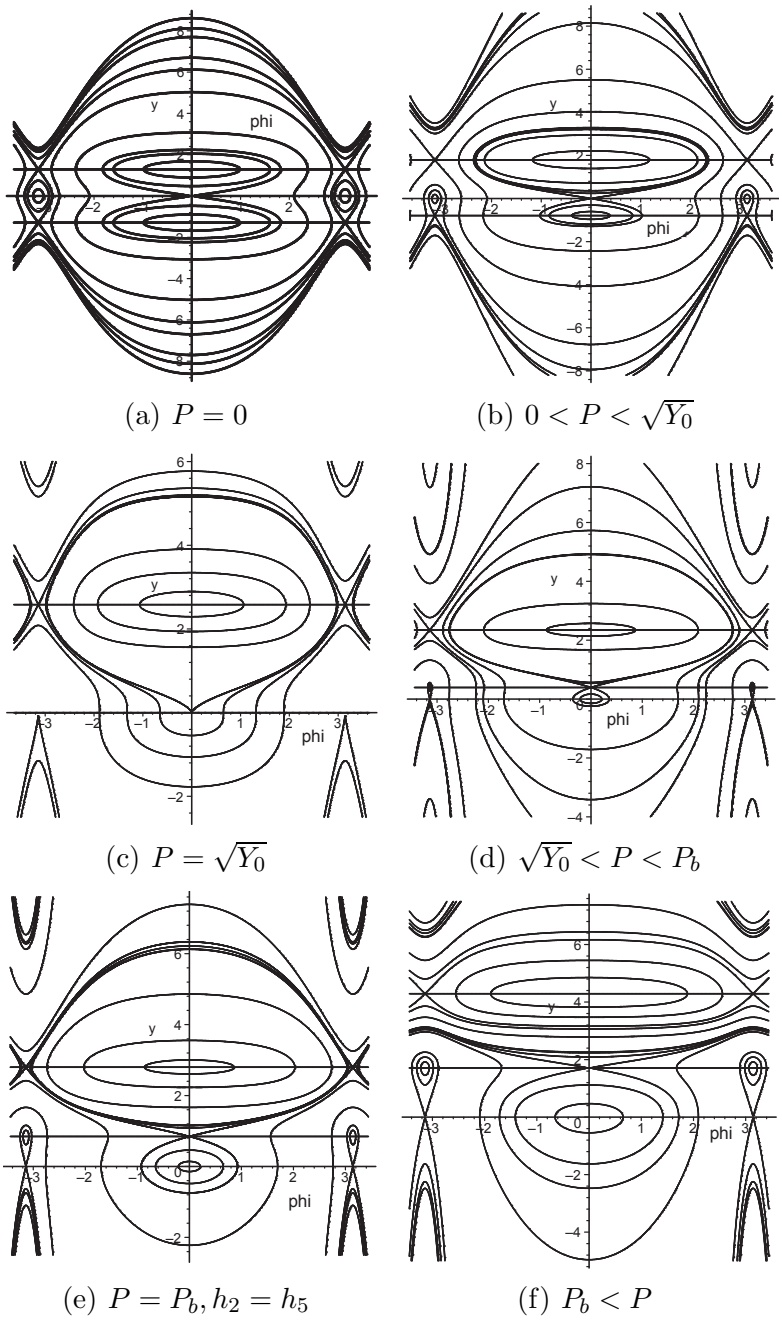

(a) $P = 0$ (b) $0 < P < \sqrt{Y_0}$

(c) $P = \sqrt{Y_0}$ (d) $\sqrt{Y_0} < P < P_b$

(e) $P = P_b, h_2 = h_5$ (f) $P_b < P$

Fig. 6. The bifurcation of phase portraits of system (10) for $0 < \mathbb{V} < 1$ and for $B = 0.9$, $\sigma = 1.5$, $\lambda = 0.03$.

The phase portraits are simple without singular lines. As shown on Fig.8, no bifurcation occurs when P or λ are varied.

In this section, we have studied the main characteristics of the phase portraits for the systems (8) and (10). We notice at this stage that the deformability parameter σ acting on substrate potential (4) does not play an important role. In fact, it only slightly and qualitatively changes the shapes of the trajectories

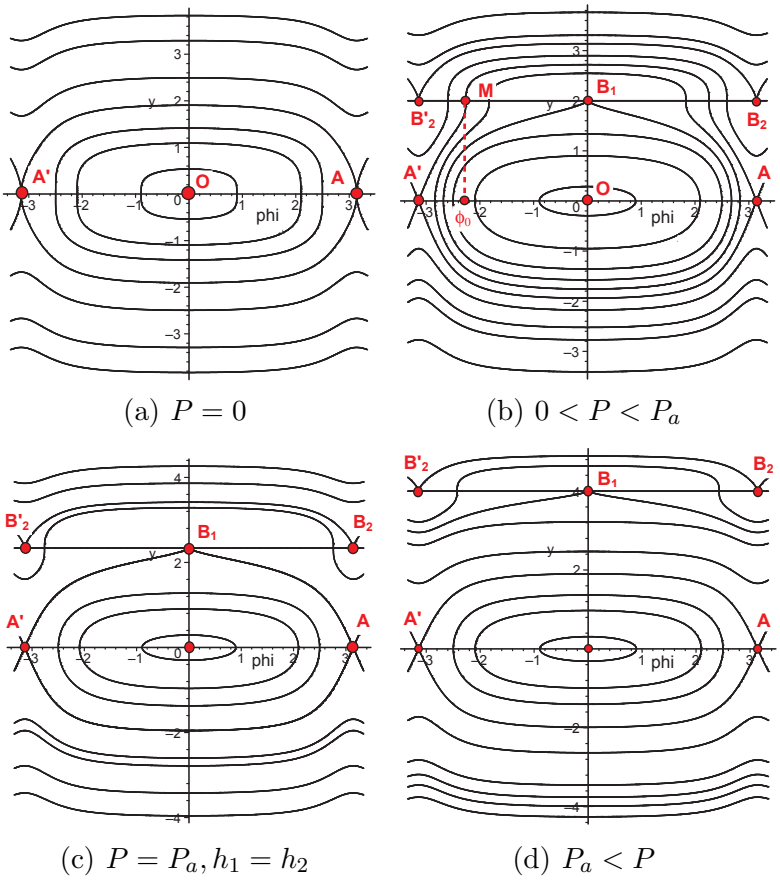

(a) $P = 0$ (b) $0 < P < P_a$

(c) $P = P_a, h_1 = h_2$ (d) $P_a < P$

Fig. 7. The bifurcation of phase portraits of system (10) for $\mathbb{V} = 1$ (sketch for any given parameter set (B, λ)).

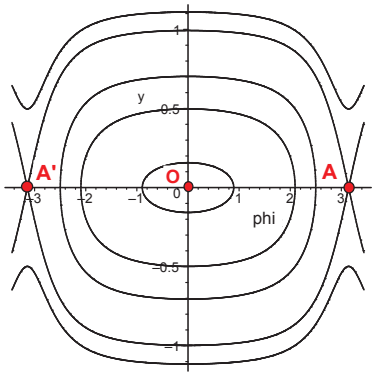

Fig. 8. Example of phase portraits of system (10) for $\mathbb{V} > 1$ (sketch for any given parameter set (B, P, λ)).

in the different phase portraits (compare Fig. 4(c) and Fig. 4(d)) where only the parameter σ is varied.

4 Dynamics of the solutions of equation (7)

In this section, we consider the solutions of equation (7) giving the wave profile $\phi(u)$ and corresponding to some trajectories of the phase portraits of section 3. For a sake of simplicity, we will consider the velocity as a decreasing parameter.

(I) **Case of supersonic velocities: $\mathbb{V} > 1$. (see Fig. 8)** .

In this case, the function $f(y)$ has no real zero. Thus, systems (8) and (10) lead both to the phase portraits of Fig. 8 for any kind of parameter set (B, P, λ).

(i) Corresponding to the family of closed orbits defined by $H(\phi, y) = h$, $h \in]-2\lambda, 0[$, there exists a family of oscillating periodic solutions of equation (7), as depicted in Fig.9(a).

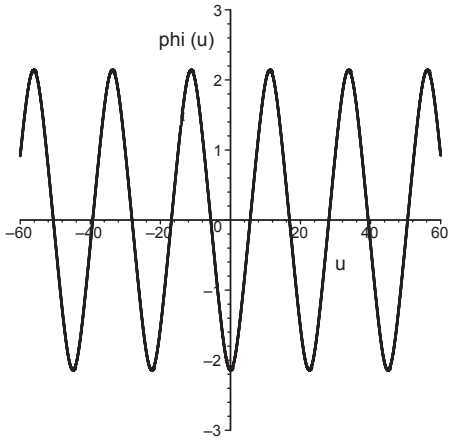

(a)

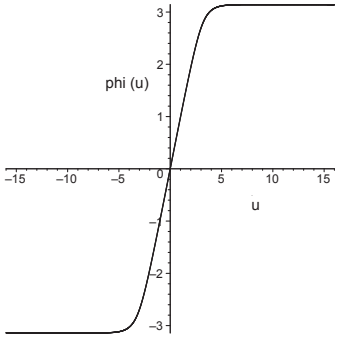

(b) Kink wave.

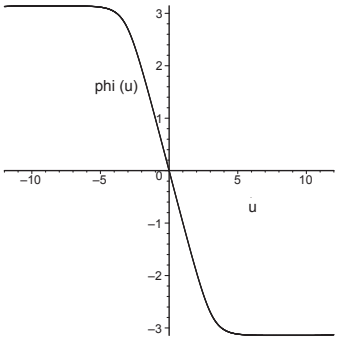

(c) Anti-kink wave

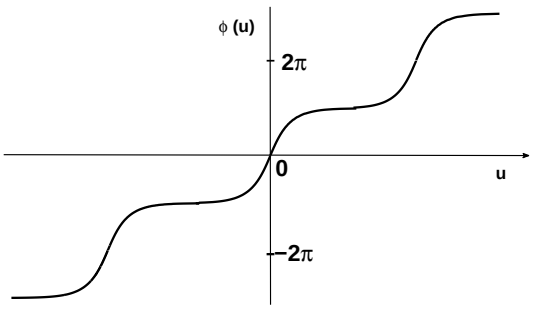

(d)

Fig. 9. Solution wave $\phi(u)$ of equation (7) corresponding to the case $V > 1$. The abscisse scale is arbitrary. [The initial values for the pair (ϕ, y) are respectively: *a*) $(-2.4, 0)$. *b*) $(-\pi, 0)$. *c*) $(\pi, 0)$. *d*) $(-3\pi, 0.1)$.]

(ii) Corresponding to heteroclinic orbits joining points A to A' in Fig.8, such as $H(\phi, y) = -2\lambda$, there exist two kink solutions as shown in Fig. 9(b) and 9(c).

(iii) Corresponding to open orbits defined by $H(\phi, y) = h$, $h \in]-\infty, -2\lambda[$, there exist rotating solutions of equation (7) with only periodic changes of positive slope y. Although these solutions may not correspond to realistic behaviors in the context of lattice systems, they are represented on figure 9(d).

(II) **Case of sonic velocities ($\mathbb{V} = 1$, see Fig. 7)**.

(II-1) If $P = 0$ (see Fig. 7(a)), there exist only the equilibrium points O, A and A', and the families of solutions for Eq. (7) are the same as the ones reported in § 4(I).

(II-2) If $0 < P < P_a$ (see Fig. 7(b)) or $P = P_a$ (Fig. 7(c)) we have $h_4 < h_1 < h_2 < 0$ or $h_4 < h_1 = h_2 < 0$ respectively.

- Corresponding to the family of closed orbits defined by $H(\phi, y) = h$, $h \in]h_2, 0[$, there exists a family of oscillating periodic solutions of Eq. (7) similar to those shown on Fig. 9(a).
- Corresponding to the family of closed orbits defined by $H(\phi, y) = h$, $h \in]h_1, h_2]$, there exists a family of oscillating periodic solutions of Eq. (7). But these orbits intersect the singular straight line $y = P$ first for $-\pi < \phi < 0$. For example, the orbit starting from the point $A'(\phi = -\pi, y = 0)$ in Fig. 7(b) intersects the singular straight line at point M. The wave profile, as shown on Fig. 10 leads to the lattice dislocation when $\phi = \phi_0$ and $y = P$. At this point, this gives rise to a breaking solutions $\phi(u)$.

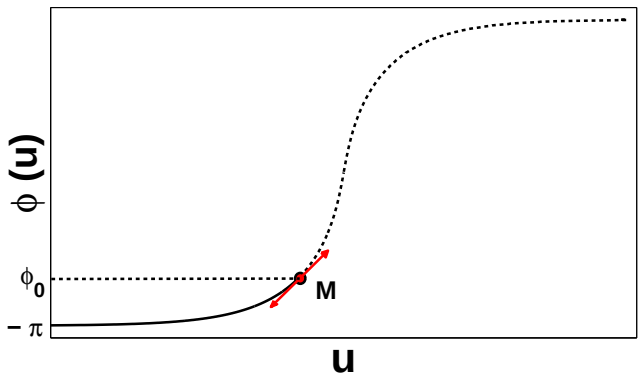

Fig. 10. Sketch of a dislocation. Starting from the point A' in Fig. 7(b), the orbit intersects the singular straight line at point M, when the slope $\dfrac{d\phi(u)}{du} = P$. (Same parameter set as for Fig. 7).

- Considering the two heteroclinic orbits linking the equi-

librium points A and A' $[H(\phi, y) = h_1]$, the upper one intersects also the singular straight line $y = P$ first for $-\pi < \phi < 0$ (behavior similar to the one depicted in Fig. 10) while the lower one is a standard anti-kink wave (similar to Fig. 9(c)).

- Corresponding to $H(\phi, y) < h_1$, there exist different families of trajectories. For the lower ones, the profiles $\phi(u)$ resemble to the curves on Fig. 9(d) while the upper ones intersect the singular straight line $y = P$ and correspond to breaking wave solution as on Fig. 10.

(II-3) $P > P_a$. In this case $h_4 < h_2 < h_1 < 0$. In addition to the previous case, we notice the presence of a heteroclinic orbit joining the points A' and A, corresponding to a kink wave solution $\phi(u)$ similar to the curve on Fig. 9(b).

(III) **Case of subsonic velocities (**$0 < \mathbb{V} < 1$).

(III-1) Let us consider first the case $P = 0$ (see Fig. 5 (a, b, c)).
Some families of orbits do not intersect the singular straight lines $y = y_1 = \sqrt{Y_0}$ and $y = y_2 = -\sqrt{Y_0}$. There are limit cycles around the equilibrium points A' or A. The corresponding wave solution $\phi(u)$ of Eq. (7) is similar to those depicted on Fig. 9(a), with only a difference concerning the ordinate values.
We notice even, when $\lambda < \lambda_b$ (Fig. 5(a)), that a kink (antikink) solution links the point O to the point $O'(2\pi, 0)$, with the corresponding wave solutions $\phi(u)$ sketched in Fig. 11. Note here the influence of parameter σ on the shape of the wave $\phi(u)$: it only concerns the width of the kink (compare Fiq. 11 (a), (b) and (d)).
The other families of orbits in this case all intersect one of the singular straight lines. They correspond thus to breaking waves solution $\phi(u)$, with the dislocation happening precisely when their slope $y = \dfrac{d\phi}{du}$ reaches either $\sqrt{Y_0}$ or $-\sqrt{Y_0}$.

(III-2) $0 < \mathbb{V} < 1$ and $P \neq 0$ (see Fig. 6(a)$\rightarrow$ 6(f)).
In this case, almost all orbits of systems (8) and (10) intersect the singular straight lines $y = P + \sqrt{Y_0}$ and $y = P - \sqrt{Y_0}$, giving rise to breaking solutions $\phi(u)$. The only difference between these waves stands on the position of the initial condition.
A few orbits do not intersect the singular straight lines. They correspond to periodic oscillations around the equilibrium points A' and A (if $P \leq \sqrt{Y_0}$) and around the equilibrium point O (if $P > P_b$). In this later case, an heteroclinic orbit linking A to A' exist, whose corresponding $\phi(u)$ is an anti-kink wave.

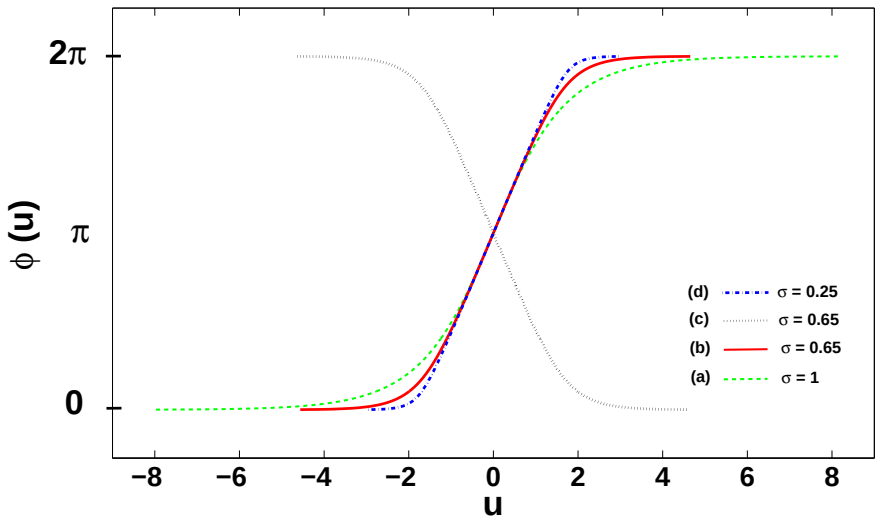

Fig. 11. The kink wave and anti-kink wave of Eq (7) for $0 < \mathbb{V} < 1$ (Parameters: $P = 0,\ \mathbb{V} = 0.2,\ B = 0.9,\ \lambda = 0.025$. For (a) , (b) and (d) $\phi(-\infty) = 0,\ y(-\infty) = 0$ but σ takes different values. For (c) $\phi(-\infty) = 2\pi,\ y(-\infty) = 0$).

5 Conclusion

In summary, we have studied the dynamic behaviors of traveling wave solutions of the generalized Frenkel-Kontorova model. Our model extends previous lattice soliton-bearing one-dimensional models discussed in the literature, by considering the contribution of anharmonic couplings. Such couplings are achieved through a non-convex interaction potential and a deformable substrate potential. In the continuum limit, a Singular Nonlinear Equation of the Second Class governs the displacement of the particles. Under different parametric conditions, we have shown that various sufficient conditions lead to the existence of a rich diversity of solitary and periodic wave solutions. Another effect is related to an opening of phase trajectories of the system taking place beyond some threshold values of the lattice parameters, and depending on the velocity of the soliton patterns. Analytical expression for the breakdown threshold has been derived although it is quite indifferent of the deformability of the substrate (σ being not a bifurcation parameter). The deformability of substrate in such model gradually has only an influence on the width of the wave solutions. The parameter P, as well as other defects, may locally influence the breakdown threshold and thus plays a major role with respect to nonlinear excitations in such systems.

The bifurcations and dynamic behaviors of traveling wave solutions can be suitable for another nonlinear wave equation. Although it is tremendously challenging to analytically determine the explicit travelling wave solutions, our preliminaries results suggest that they can be combined with a bifurcation method in order to provide an insight of at least implicit solutions. The

findings reported in this paper might be of critical impacts in several areas of applied sciences. For instance, they can help to explain the formation of cracks originating from dislocations that are observed in semiconductor heterostructures [1,14–16]. Moreover, they can help to better understand the break up (rupture) of a stretched polymer chain by pulling and its relation to soliton destruction [22].

References

[1] Braun OM, Kivshar YS. "*The Frenkel-Kontorova Model, Concepts, Methods, and Applications*". Springer-Verlag: Heidelberg New York; 2004.

[2] Yuan XP, Zheng ZG. "*Nonlinear Dynamics of a Sliding Chain in a Periodic Potential*". Chin Phys Lett (2007); **24**: 2513.

[3] Vanossi A, Braun OM. "*Driven dynamics of simplified tribological models*", J Phys: Condens Matter (2007); **19**: 305017.

[4] Li BW, Wang L, Casati G. "*Negative differential thermal resistance and thermal transistor*". Appl Phys Lett (2006); **88**: 143501.

[5] Li BW, Lan JH, Wang L. "*Interface Thermal Resistance between Dissimilar Anharmonic Lattices*" Phys Rev Lett (2005); **95**: 104302.

[6] Hu B, Yang L, Zhang Y. "*Asymmetric Heat Conduction in Nonlinear Lattices*". Phys Rev Lett (2006); **97**: 124302.

[7] Martínez PJ, Chacón R. "*Taming Chaotic Solitons in Frenkel-Kontorova Chains by Weak Periodic Excitations*". Phys Rev Lett (2004); **93**: 237006.

[8] Chacón R, Martínez PJ. "*Controlling Chaotic Solitons in Frenkel-Kontorova Chains by Disordered Driving Forces*". Phys Rev Lett (2007); **98**: 224102.

[9] Martínez PJ, Chacón R. "*Taming Chaotic Solitons in Frenkel-Kontorova Chains by Weak Periodic Excitations*". Phys Rev Lett (2004); **93**: 237006.

[10] Xu H, Chen WZ, Zhu YF. "*Influence of the bond defect in driven Frenkel-Kontorova chains*". Phys Rev B (2007); **75**: 224303.

[11] Tchakoutio Nguetcho AS, Bogning JR, Yemele D, Kofane TC. "*Kink compactons in models with parametrized periodic double-well and asymmetric substrate potentials*". Chaos, Solitons and Fractals (2004); **21**: 165.

[12] Tchakoutio Nguetcho AS, Kofane TC. "*Soliton patterns and breakup thresholds in hydrogen-bonded chains*". Eur Phys J B (2007); **57**: 411.

[13] Milchev A, Markov I. "*The effect of anharmonicity in epitaxial interfaces: I. Substrate-induced dissociation of finite epitaxial islands*". Surf Sci (1984); **136**: 503.

[14] Braun OM, Kivshar YS. "*Nonlinear dynamics of the Frenkel-Kontorova model*". Phys Rep (1998); **306**: 1.

[15] Milchev A. "*Solitary waves in a frenkel-kontorova model with non-convex interactions*". Physica D (1990); **41**: 262.

[16] Malomed BA, Milchev A. "*Interaction of dislocations with a local defect in an atomic chain with a nonconvex interparticle potential*". Phys Rev B (1990); **41**: 4240.

[17] Li Jibin. "*Singular Nonlinear Traveling Wave Equations: Bifurcations and Exact Solutions*". Beijing: Science Press; (2013).

[18] Li Jibin, Shenjianwei. "*Travelling wave solutions in a model of the helix polypeptide chains*". Chaos Solitons Fractals (2004); **20**: 827.

[19] Li Jibin, Zhao Xiaohua, Chen Guanrong. "*On the Breaking Property for the Second Class of Singular Nonlinear Traveling Wave Equations*". Int J of Bifurcation Chaos (2009); **19**: 1289.

[20] Asit Saha. "*Bifurcation of travelling wave solutions for the generalized KP-MEW equations*". Commun Nonlinear Sci Numer Simul (2012); **17**: 3539.

[21] Fang Yana, Haihong Liub, Zengrong Liu. "*The bifurcation and exact travelling wave solutions for the modified BenjaminBonaMahoney (mBBM) equation*". Commun Nonlinear Sci Numer Simul (2012); **17**: 2824.

[22] Paturej J, Milchev A, Rostiashvili VG, Vilgis TA. "*Thermal degradation of unstrained single polymer chain: Non-linear effects at work*". J Chem Phys (2011); **134**: 224901.